Permafrost, Phillips, Springman & Arenson (eds)
© 2003 Swets & Zeitlinger, Lisse, ISBN 90 5809 582 7

A comparison of snow melt at three circumpolar sites: Spitsbergen, Siberia, Alaska

J. Boike
Alfred Wegener Institute for Polar and Marine Research, Potsdam, German

L.D. Hinzman & P.P. Overduin
Water and Environmental Research Center, University of Alaska, Fairbanks, Alaska, USA

V. Romanovsky
Geophysical Institute, University of Alaska, Fairbanks, Alaska, USA

O. Ippisch & K. Roth
Institute for Environmental Physics, University of Heidelberg, Heidelberg, Germany

ABSTRACT: Spring snow ablation is modelled at three patterned ground sites in Spitsbergen, Siberia and Alaska for 1999 and 2000 using a volume energy balance model. The sites on Spitsbergen and Alaska have a thick snow cover, while the Siberia snow pack is thin and spatially heterogeneous. The main components of the energy balance are atmospheric fluxes (radiative, turbulent), but their percentage differs significantly between sites. On Spitsbergen and Siberia ablation energy is mostly provided by net radiation, on Alaska by sensible heat and net radiation. Almost 50% of available energy is lost by sublimation in Siberia. The loss of heat into the ground is the smallest component in the balance. The physical properties of snow, soil and surface vegetation determine the ground heat flux resulting in a maximum loss of 18% at the Siberia and minimum of 6% at the Alaskan site.

1 INTRODUCTION

Snow has an important role information of patterned ground. For example, snow melt water infiltration into cracks creates polygonal patterned ground. Snow differs spatially over patterned ground in thickness and physical properties. This has two important consequences: (i) ground heat transfer varies spatially and (ii) snow melt varies spatially and temporally.

By comparing surface energy balance components, the control mechanism at the local scale (such as surface characteristics) are examined relative to the larger scale factors (such as climate). We compare the energy balance at three patterned ground sites during one snowmelt season: Ny-Ålesund (Spitsbergen, 1999), the Lena River Delta, (Siberia, 1999) and Ivotuk (Alaska, 2000). Continuous permafrost underlies all these sites under the influence of different climates. The climate at each site for the years studied is not extreme when compared to the long term record.

2 METHODS

A volume energy balance model between snow surface and permafrost table is applied to calculate turbulent heat fluxes, heat flux by rain and heat flux of the ground and snow (Boike et al. 2003):

$$Q_n + Q_h + Q_e + Q_r = \Delta H_g + \dot{\Delta} H_l + \dot{\Delta} H_s + Q_m \quad (1)$$

where Q_n is the net radiation balance, Q_h and Q_e are turbulent fluxes of sensible and latent heat, Q_r is the heat flux supplied by rain, ΔH_g and $\dot{\Delta} H_s$ are the changes of sensible heat in the soil and the snow, respectively, and ΔH_l is the change in latent heat of the ground. The latent heat of the snow pack, Q_m, is the remainder in the balance. For $Q_m > 0$, melting is expected while for $Q_m < 0$, freezing and recrystallization are expected. Atmospheric fluxes (defined here as Q_n, Q_h, Q_e and Q_r) towards the snow pack are defined as positive (energy gain), away from it as negative. Net radiation is measured at all sites using Q7 or NR LITE net radiometers. The bulk aerodynamic method is used for the calculation of atmospheric sensible and latent heat fluxes using hourly measurements of air temperature, humidity, wind speed and snow depth. The heat flux by rain is computed using rainfall rate and air temperature. Ground and snow heat fluxes are calculated as hourly changes of the soil's and snow's sensible and latent heat using hourly temperature and volumetric liquid water content data. Ground heat flux below the instrumented soil volume is ignored because the temperature gradient at the permafrost table is very close to zero. Snow heat flux is only calculated for the Bayelva site since automatic snow temperature and liquid water content data are available. Details on the method and the calculations are provided in Boike et al. (2003) and Kane et al. (1997). Surface roughness z_o is used as a tuning parameter at the Ivotuk and Bayelva site since no wind profile measurements are available. At the Bayelva site, turbulent heat fluxes agree well with fluxes calculated from the aerodynamic profile method utilizing two level measurements at a nearby site (Semandeni-Davies et al., in prep.). For the Samoilov site z_o is calculated using detailed topographic survey data from 1999 following the method of Lettau (1969). Calculated roughness lengths are 0.0001 m for the Bayelva site, 0.001 m for Ivotuk and 0.01 m for Samoilov. Similar roughness lengths are well-documented over snow and support the distinct surface characteristics. The Samoilov snow cover is thin, heterogeneous and polygonal ridges protrude through the snow thus increasing z_o. A low z_o at the Bayelva site is the result of a very smooth snow surface and a large fetch. The z_o value for Ivotuk lies between these two extremes, reflecting an unscoured surface with a "felt-like structure" (M. Sturm, pers. comm.).

3 STUDY SITES

IVOTUK is located on the North Slope in Alaska, on the central southern coastal plains north of the Brooks Range (68°29′N, 155°44′W). Mean air temperatures recorded at the site in 1999 are −26 and 11°C for January and July. Summer rainfall (May–September) totals about 180 mm. Snow starts to accumulate at the end of September, reaching a total depth of about 65 cm in May before snow melt. The snow typically consists of 2/3 of depth hoar and 1–2 relict wind crusts. Mid-winter melt events are quite rare and usually only warm the near surface snow. The study site is located on typical arctic tussock tundra terrain with 0–1% slope and poor drainage.

The loamy soil is characterized as "Ruptic-Histic Aquiturbel" (organic ruptured by frost heave, reducing conditions, cryoturbation). The upper 30 cm are peat and peat muck. Permafrost is encountered at about 68 cm depth and the mean annual temperature at the top of the permafrost is −2.8°C from October 1, 1999 to September 30, 2000.

The BAYELVA catchment is located about 3 km from Ny-Ålesund, Spitsbergen (78°55′N, 11°50′E). Continuous permafrost in this region underlies coastal areas to depths of about 100 m and mountainous areas to depths greater than 500 m. The North Atlantic Current warms this area to average air temperatures around −13 and 5°C in January and July and provides about 400 mm annual precipitation falling mostly as snow between September and May. Our study site is located at about 25 m above mean sea level, on top of a small hill covered with unsorted circles. Snow height data collected at the site show that snow accumulation begins in October, but is interrupted by winter melt events, creating internal ice lenses and/or basal ice (Boike et al. 2003).

The end of winter snow thickness is about 85 cm and snow melt typically starts around late May.

Soil instruments are installed in the bare inner part of one circle, consisting of silty clay with interspersed

Figure 1. Tussock tundra terrain at the study site at Ivotuk, Alaska. The Brooks Range is visible in the background.

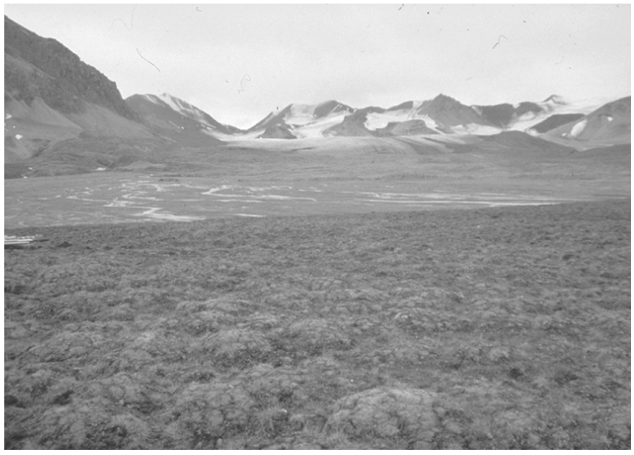

Figure 2. The Bayelva study site on Spitsbergen. The site is covered with unsorted circles ~1 m in diameter. Bayelva river and Brøggerbreen glacier are in the background.

Figure 3. Polygonal patterned ground at the study site on the island Samoilov in the Lena River Delta, Siberia.

stones. The average annual temperature at the top of the permafrost is −2.9°C. (October 1, 1998 to September 30, 1999).

SAMOILOV is one of the 1500 islands of the Lena Delta, located in one of the main river channels in the southern part of the delta (72°N, 126°E). Continuous permafrost underlies the area to about 400–600 m. This area has the most extreme climate (coldest air temperature and lowest precipitation). Long term mean air temperatures recorded at Tiksi are −33.3 and 7.0°C for January and July and annual total precipitation is around 125 mm, but winter snowfall is low (<40 mm). On the island, strong winds redistribute snow, resulting in bare surfaces on polygonal apices and snow-filled polygonal centers with up to 43 cm snow. Strong winds lead to aeolian sedimentation of sands. The climate station is situated on polygonal patterned ground (low-centered polygon) on peatish sand deposits of an ancient delta flood plain. The waterlogged soils are classified as "Fluvaquentic Fibristils" and the tundra vegetation consists of 80% bryophytes. The mean annual temperature at the top of the permafrost is −10.1°C (October 1, 1998 to September 30, 1999), about 8°C colder compared to Ivotuk and Bayelva. Soil instruments are installed within the polygon's apex.

4 RESULTS

4.1 *Comparison of measured and modelled changes in snow water equivalent (SWE)*

Dingman (1994) divides the snow ablation period into warming, ripening and output phases. Melt water flowing out of the snow pack is only created during the output phase; during the warming and ripening stage the snow densifies and compacts due to surface melt and snow internal processes, such as percolation of water and subsequent growth of larger snow grains. Boike et al. (2003) show for the Bayelva site that the energy balance model is capable of distinguishing these two periods. When Q_m values become positive, the pre-melt period (warming and ripening of snow) is completed and runoff (output) starts. Measured and modelled ablation rates are in good agreement for the melt period for the examined years of 1999 and 2000 (Boike et al. 2003). A good agreement between measured and modelled snow ablation rates is also found for the melt period for the Ivotuk site starting on May 31, 2000 (Figure 4). Pre melt snow bulk density is about $250\,kg\,m^{-3}$ increasing to about $350\,kg\,m^{-3}$ towards June 4 (M. Sturm, pers. communication). Thus, a density of $350\,kg\,m^3$ is used for snow water equivalent calculation during the melt period.

At the Samoilov site, a very heterogeneous snow cover, redistribution of snow due to high wind speeds and few manual measurements of snow depth (the automated snow sensor did not produce reliable measurements due to the very thin snow cover) make the comparison between modelled and measured SWE rates difficult. Measured decrease of SWE in the field

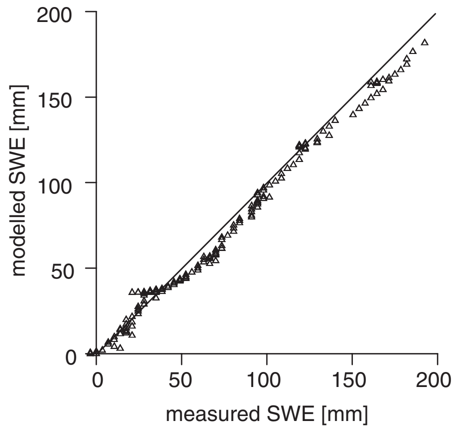

Figure 4. Comparison between measured and modelled cumulative changes in SWE for the melt period for the Alaska site at Ivotuk. Measured SWE was calculated using the decrease of snow height measured by the snow sensor and an average measured snow density of $350\,kg\,m^{-3}$. Modelled melt rates are calculated using Q_m from the energy balance.

at various sites agrees reasonably well with modelled results. The energy balance model calculates a total of 86 mm snow ablation from May 11 to 25, 1999. During the pre-melt (until May 18) 8 mm snow sublimates while minimum and maximum decrease in measured field SWE are 6 and 26 mm using an average measured snow density of $290\,kg\,m^{-3}$. Snow profiles and field data support the observation that sublimation is the dominant process during the pre-melt period. During the melt period, a total of 61, 81 and 90 mm SWE ablate at the stakes located at 2, 2.50 and 4 m along the transect (distance to apex), which are similar to the 78 mm SWE obtained from model estimates.

4.2 *Comparison of snow thermal properties before melt*

Mid winter warming events, and possibly rain, promote formation of internal ice lenses or basal ice in the snowpack on Bayelva, depending on thermal state of snow (Boike et al. 2003). A typical pre-melt snow profile is shown in Figure 5. Snow densities increase to an average of $450\,kg\,m^{-3}$ towards the melt period. In Siberia, a 24 cm depth hoar layer, with a windslab 17 cm above the ground surface, and 8 cm of overlying snow comprise the snow profile. A surface crust and hardened layers within the snow profile contain a large amount of aeolian sediments and indicate high wind speeds (Figure 5). Large depth hoar crystals with grain sizes larger than 3 mm are the result of steep temperature gradients between soil and air and their associated vapor pressure gradients. In addition, the long grass tundra vegetation promotes depth hoar formation by preserving a loose, aerated layer at the snow cover base.

The Ivotuk profile (May 11, 2000) consists of a large depth hoar layer of 38 cm overlain by a further 32 cm of mixed snow types. Thin ice layers and glaze crusts are present in this mixed layer.

4.3 *Snow melt, Bayelva 1999*

The process of snow ablation for the years 1999 and 2000 has been examined in detail in Boike et al. (2003). In 1999, snow ablation takes 47 days: surface melt and snow internal processes (ripening) reduce the snow pack thickness (but not SWE) from May 5 until June 7, after which output is produced within 14 days. Rain on snow events occur frequently, but do not contribute substantial energy. The cumulative sum of energy balance components during snow ablation in 1999 is shown in Figure 6. The dominant source of energy for melt is provided by Q_n. Evaporation and sublimation use about 30% of Q_n. Q_r and ΔH_s are insignificant. Due to the long ablation period, $\Delta H_g + \Delta H_l$ are a significant energy sink, using 30% of total energy supplied by Q_n. The snow melt at this site in 2000 is similar and thus is not discussed here.

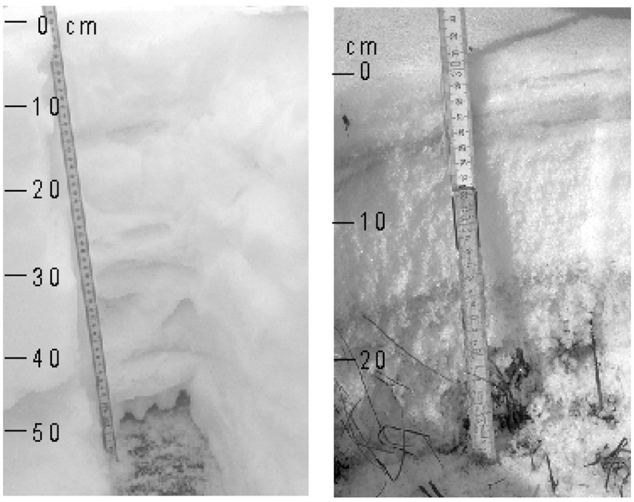

Figure 5. Contrasting pre-melt snow profiles in 1998 at the Bayelva site (left) and in 1999 at the Samoilov site (right); the latter is taken within the polygon's snow filled center. The snow at Bayelva has a higher density, several internal ice layers and a basal ice layer. The snow on Samoilov consists mainly of very loose, large-grained depth hoar. Visible are also two hardened, sediment rich layers.

4.4 *Snow melt, Samoilov 1999*

The polygon pattern results in a highly variable microtopography and snow depth. The snow cover on the polygon's apexes ranges between 0 and 10 cm, while the center has a snow filling of up to 43 cm. Figure 6 shows the cumulative energy fluxes and ablation of snow at several positions along a transect extending from the polygon's apex to the center.

Throughout the winter and during the pre-melt period, snow exclusively sublimates (sublimation is possible due to high wind speeds) exposing the polygon ridges. The air temperature remains far below 0°C (Boike & Becker 2000), wind speeds can average a maximum up to $15\,\mathrm{m\,s^{-1}}$, increasing the turbulent losses through latent heat.

One warming event on May 17 melts the upper 5 cm of the snow, but snow temperatures are still far below freezing, -13°C at the bottom of the snow. Infiltration of surface melt and subsequent densification is indicated by an increase of snow density (from 250 to $290\,\mathrm{kg\,m^{-3}}$) and homogenization of snow layers. Melt starts around May 18 when Q_m becomes positive with Q_n providing the major source.

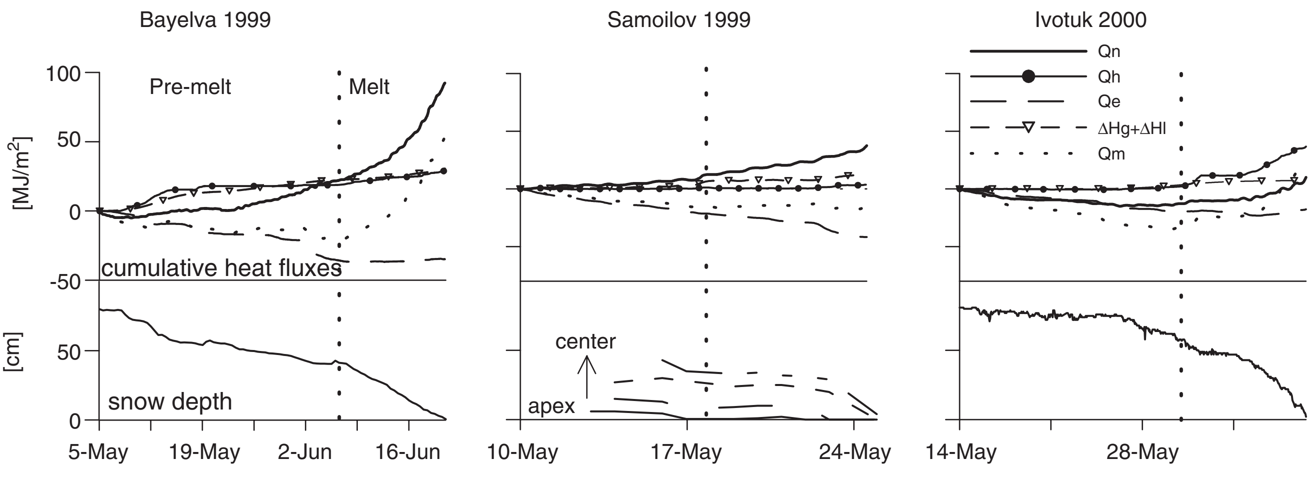

Figure 6. Cumulative sum of heat fluxes and snow depth for the three study sites during the snow ablation periods in 1999 for the Bayelva and Samoilov sites and 2000 for the Ivotuk site. The ablation period is divided into pre-melt and melt periods when Q_m values become positive. The sensible and latent heat of the snow pack is only calculated for the Bayelva site. Q_r and ΔHs are negligible and not shown here.

4.5 *Snow melt, Ivotuk 2000*

During the 17-day pre-melt period (May 14–30, 2000) the snow cover decreases by about 28 cm, caused by compaction due to surface melt (event with a positive air temperature on May 16) and snow internal processes. Continuous surface melting starts on May 26, suggested by positive air temperatures and a steep increase in snow temperatures (Hinzman & Peltier 2001). Starting on May 31, Q_m values increase, indicating a ripe snowpack. This is corroborated by snow temperatures: isothermal conditions around 0°C within the snow pack permit free percolation of melt water to the ground (Hinzman & Peltier 2001). A period of cold sub zero air temperatures between June 1 to 4 interrupts the snow melt (Q_m plateau). This plateau of no SWE change is depicted by the model. After this, a pronounced increase in air temperature and net radiation concomitant with a drop in air humidity produces steadily increasing Q_m. The energy for warming and ripening of the snow is derived from Q_n and Q_h. During the first 6 days of the melt phase, the main energy source is provided by Q_h, but with progress of melt, Q_n becomes more important. As winds cross the Brooks Range to the south of the site, the air becomes drier as it rises and warmer as it descends, thus providing energy for Q_h.

5 COMPARISON OF ENERGY BALANCE COMPONENTS

The percentage of energy balance components for the three sites is presented in Figure 7. Source pies represent the total cumulative positive energy fluxes provided by the energy balance components, whereas sink pies represent negative totals. Pie size is proportional to the total amount of heat transferred and reflects the duration of the total ablation period: 47 days and $222 \cdot 10^6$ MJ m^{-2} at the Bayelva site, 27 days and $123 \cdot 10^6$ MJ m^{-2} at Ivotuk and 15 days and $98 \cdot 10^6$ MJ m^{-2} at Samoilov. There are significant differences between the energy distributions. Melt energy at the Bayelva and Samoilov sites is largely provided by Q_n, while almost half of the melt energy at the Ivotuk site comes from Q_h. Q_e is a small source for melt via condensation at the Bayelva and Ivotuk site. $\Delta H_g + \Delta H_l$ are a small source of heat only at the Samoilov site (3%), through the infiltration and subsequent freezing of snow melt water at this apex site. The energy transferred into warming and ripening during the pre-melt period is largest at Bayelva and Ivotuk due to a thick snow cover in both locations. The biggest difference between the sinks of the energy balance of the three sites is the dominance of sublimation as energy sink in Samoilov and differences in ground heat flux. The former is a result of high wind speed in Samoilov. At Ivotuk the ground heat flux is lowest (6%) due to low thermal gradient across the snow pack and the insulating properties of the snow and upper soil horizons: a 38 cm thick depth hoar layer and deep snow profile (70 cm) plus a thick moss layer insulate the soil better at this site. The ground heat flux at the Bayelva and Samoilov site is similar, 17% and 18% respectively. At the Samoilov site, this is the result of a large thermal gradient and a very thin or absent snow cover on the polygonal ridges. In contrast, the snow cover at the Bayelva site is thick (~80 cm), but depth hoar – if present – is limited to a few centimeters. In addition, the lack of an insulating organic surface layer permits heat transfer across the mineral soil-snow interface.

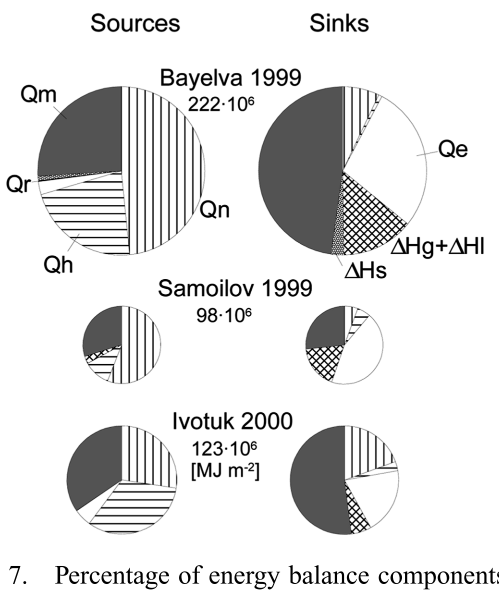

Figure 7. Percentage of energy balance components during the snow ablation periods for the three sites. The size of the pies is relative to the total amounts of energy transferred [MJ m^{-2}].

6 SUMMARY

Our energy balance method shows differences between microclimate and soil material effects on heat and mass transfer to the soil during the snow melt period. Climate affects the snowmelt period primarily via differences in snow pack and by whether atmospheric radiative or turbulent fluxes prevail in determining melt energy. Bayelva and Samoilov, both located close to the sea, experience predominantly radiative melting. Local phenomena, such as the orographic influence of the Brooks Range in Ivotuk, increase the percentage of sensible heat flux.

The sandy material at the Samoilov site is prone to deep infiltration, and the observed large thermal gradient promotes ice wedge growth though the refreeze of snow melt water. The micro-topography of the ice wedge form leads to its further development by moving water within the apex towards the site of wedge growth.

ACKNOWLEDGEMENTS

We gratefully acknowledge financial support from the Deutsche Forschungsgemeinschaft, the European Union and a research grant awarded to Julia Boike by the Deutsche Akademie der Naturforscher Leopoldina. Essential logistic support was provided by the German and the Norwegian Research Stations in Ny-Ålesund and U.S. National Science Foundation Arctic System Science Program (Grant Numbers OPP – 9818066 and OPP – 9870635).

REFERENCES

Boike, J., Roth, K. & Ippisch, O. 2003. Seasonal snow cover on frozen ground: energy balance calculations of a permafrost site near Ny-Ålesund, Spitsbergen. *J. of Geophysical Research- Atmosphere*, in press.

Boike, J. & Becker, H. 2000. Thermal and hydrologic dynamics of the active layer. In Rachold & Gregoriev. Reports on Polar Research: Russian-German Cooperative System Laptev Sea 2000 (354), 25–28.

Dingman, S.L. 1994. *Physical Hydrology*, New Jersey: Prentice Hall.

Hinzman, L.D. & Peltier, B. 2001. North American Arctic Snowmelt Season, Spring 2000 http://www.uaf.edu/water/projects/Snowmelt2000/CD/CDBrowser.htm.

Kane, D.L., Gieck, R.E. & Hinzman, L.D. 1997. Snowmelt modeling at small Alaskan arctic watershed. ASCE Journal of Hydrologic Engineering. 2(4), 204–210.

Lettau, H. 1969. Note on aerodynamic roughness-parameter estimation on the basis of roughness element description. *J. of applied Meteorology* 8: 828–832.

Semandeni-Davies, A., Maréchal, D., Bruland, O., Kodama, Y. & Sand, K. 2003. Latent heat flux estimation over a melting Arctic snow cover, Svalbard. Manuscript in preparation.